Can fibrous mats outperform current ultrafiltration and mcirofiltration membranes?

Hasin Feroz[1], Michelle Bai[2], HyeYoung Kwon[1], John Brezovec[1], Jing Peng[3], and Manish Kumar[*]

[1]Department of Chemical Engineering, The Pennsylvania State University, Pennsylvania, USA

[2]Department of Chemical Engineering, Department of Biomedical Engineering, Carnegie Mellon University, Pennsylvania, USA

[3]Department of Environmental Systems Engineering, The Pennsylvania State University, Pennsylvania, USA

*Corresponding Author, Department of Chemical Engineering, The Pennsylvania State University, Pennsylvania, USA

43 Greenberg Building, University Park, PA 16802, USA. Phone: +1 814 865 7519. Email: manish.kumar@psu.edu

Abstract

Ultrafiltration (UF) and microfiltration (MF) membranes have important applications in separations relating to proteins, pharmaceutical products, viruses, food and beverages, water treatment and sterilization. Although, phase inversion membranes have been used for MF and UF applications for decades, there has been an increase in interest in using electrospun fibrous mats as MF/UF membranes instead. While the selectivity-permeability trade-off for conventional phase-inversion UF membranes is now established, such an understanding for phase-inversion MF membranes and for fibrous mat membranes does not exist. Here, we report the first preliminary selectivity-permeability trade-off for commercially available MF membranes. We also describe a theoretical framework that can be used to evaluate the performance of fibrous mats. Mats consisting of a random array of nanofibers were modeled with a gamma pore size distribution based on previous work. The pore size distribution of the mat was related to the physical properties of the mat such as porosity, fiber diameter, density, areal density, and mat thickness. This distribution was then used in conjunction with a procedure developed by Zydney and coworkers to conduct *a priori* predictions of the performance of fibrous mat UF and MF membranes in terms of their hydraulic permeability and selectivity to the model solutes, 3.65 nm radius bovine serum albumin (BSA) and 100 nm radius microspheres, respectively. We compared the performance of modeled mats of varying properties with the selectivity-permeability trade-off curve of current UF and MF membranes. A surprising finding was that, as modeled, the performance of fibrous mat membranes can only surpass that of current UF and MF membranes under very limited conditions. These conditions include very low fiber sizes of ~ 2 nm and ~70 nm and membrane thicknesses of < 100 nm and <1000 nm for UF and MF membranes, respectively. These metrics are challenging to achieve under currently used manufacturing conditions.

Introduction

Commercial ultrafiltration (UF) and microfiltration (MF) membranes are an established separation technology for several applications including water treatment, dairy applications, dialysis, protein separations and virus removal.[1-8] Conventional MF membranes formed by phase inversion are symmetric in that there is little difference in pore structure along the depth of the membrane, which is in the order of ~100 μm. Most commercial UF and some of the higher permeability MF membranes, rely on an asymmetric structure created by the phase inversion process leading to a thin (100 - 5000 nm) "active" layer deposited on or gradually expanding into a more open matrix. This design has endured for decades and has been improved upon to establish a highly stable structure. However, there exists in commercial UF and MF membranes a trade-off between selectivity and permeability[9] that is a significant barrier to further development of these membranes. Based on the trade-off between permeability and selectivity an upper bound was proposed for conventional UF materials by Zydney and coworkers (reproduced in **Figure 1**). The "upper bound", proposed by Zydney and coworkers, provides an excellent baseline for comparison of actual improvements that new UF membrane materials can provide. We obtained a similar upper bound for commercially available MF membranes using the same model and experimental work for a larger solute **(Figure 1**).

New developments in electrospinning polymers have produced a technology where a variety of materials, including polymers, such as polyacrilonitrile (PAN) and polyethersulfone (PES) can be spun into fibers, which can then be laid down as mats.[6-8,10,11] Other methods of depositing nano and microfibrillar mats[12,13] such as those using cellulose microfibrils and carbon nanotubes (CNT) [14] have also been developed to create high performance materials. Electrospinning has the unique advantage of greater control over mat and fiber thickness and pore size and size distribution depending on electrospinning conditions, e.g., polymer concentration, solution composition, and voltage applied.[6-8] Electrospun membranes typically have higher surface area to volume ratio and high tensile strength, making them ideal for filtration applications-particularly for MF.[6-8,10,11] These mats have been proposed as alternative filtration materials for use as microfiltration (MF)[7,15] and UF[16] membranes and as support layers in nanofiltration (NF)[17] and reverse osmosis (RO) membranes. Despite claims of improved permeability, selectivity and fouling resistance, a fundamental understanding of the performance improvements that can be

expected from these novel materials has not been investigated systematically. Literature-reported electrospun membranes (those without post-processing) and their performance as MF membrane for 0.2 μm diameter particles are summarized in **Figure 2**. Here, we see that literature reported electrospun membranes seldom exceed the commercially available membranes in performance as evaluated using the permeability-selectivity trade-off curve. This study focused on developing a method to conduct *a priori* predictions of structural and transport properties of electrospun mats made from different materials and to determine key parameters that could enhance their application for commercial MF and UF applications.

The approach developed here for the analysis of nanofibrous mats as filtration materials is based on extensive studies that originated in the field of modeling the structure of paper and has since been proposed for electrospun/nanofiborus materials as filters, reinforced composites and scaffolds for tissue culture.[18-20] Paper has been successfully modeled as a mat of randomly oriented or isotropically distributed cellulose fibers over the years. This work was pioneered by the Sampson group at the University of Manchester.[21,22] We utilized this knowledge to create pore size distributions of fibrous mats of different parameters and combined it with the approach proposed by Zydney and coworkers to develop selectivity and permeability trade-off curves using bovine serum albumin (BSA) and 0.2 μm polystyrene particles as model solutes for UF and MF applications, respectively.

A step-by-step method was developed to calculate mean pore radius and pore size distribution (probability density of pore radii) given density of material, porosity, fiber diameter, and areal density (g/m^2). Areal density can be related to number of layers and thickness of the mats formed. Once these properties are determined, permeability and selectivity calculations are made based on assuming a gamma type pore size distribution, as proposed by Eichhorn and Sampson.[19]

Further, to compare these materials to the current state-of-the-art UF and MF membranes, selectivity-permeability trade-off curves were constructed for a variety of materials and porosities. Bovine serum albumin (BSA), a common model protein for UF applications, was used to model selectivity and permeability through cellulose nanofiber mats of different designs. It was seen that to approach and surpass the selectivity and permeability of current UF

membranes for BSA molecules, the thickness of a highly porous (porosity ~ 0.9) nanofiber mat has to be in the range of a few hundred nanometers. Both the porosity and density of the fibers (representing different materials) have minor impacts on this conclusion. Also to make such layers possible, very small diameter nanofibers have to be utilized (0.7 – 5 nm). These fiber diameters are smaller than the range currently considered to be accessible using conventional electrospinning techniques (10-1000 nm)[10] even though some reports exist of electrospun fibers of smaller diameters.

Literature reports on filtration experiments with 0.2 μm polystyrene microspheres through polyacrylonitrile (PAN) electrospun mats of different designs for MF applications were used to construct a selectivity permeability curve for current fibrous mat membranes. Experiments were conducted with 0.2 μm polystyrene microspheres on a range of current 0.2 μm pore size membranes to obtain a selectivity permeability curve for current MF membranes. Additional modeling revealed that for a highly porous (porosity ~0.8) electropsun mat to outperform commercially available MF membranes, we need fibers in the order ~70 nm and mats of thicknesses ~ 1000 nm. While 70 nm diameter fibers can be readily achieved using current electrospinning technology, obtaining relatively thin mats of ~1000 nm (~ 1 micron) is challenging for practical applications as most literature reported mats are in the order of tens of microns.[6-8]

Thus, somewhat counter to the current narrative of fibrous mats in general and electrospun mats in particular, a careful evaluation of fibrous mats shows that such materials could outperform current state-of-the-art UF and MF membranes only under very limited conditions. This work provides a evaluation framework to inform future work with next generation fibrous mat membranes.

Theory

The following paragraphs describe our approach to calculate specific membrane properties such as the average pore size, pore size distribution, and corresponding permeability and selectivity

for fibrous mats. These properties can be determined based on the material density, fiber diameter, membrane porosity, and mat areal density (g/m^2) where areal density is related to number of layers and thickness of the mats formed.[19] The procedure adapted from Eichhorn and Sampson, was used to determine the structural properties of fibrous mats assuming isotropic distribution of fibers.[19] The resulting pore size and pore size distribution was used to determine permeability and selectivity for a model solute using techniques described by Mehta and Zydney.[9]

For a material with porosity (ε) greater than 0.3, the mean pore radius ($\bar{r}_{2D}$) can be determined from the fiber width (ω) as follows.[19,20]

$$\bar{r}_{2D} \approx \frac{\sqrt{\pi}}{4}\left(\frac{\pi}{2log(1/\varepsilon)} - 1\right)\omega \quad (1)$$

Assuming a gamma distribution, which was found to be appropriate for layers of randomly oriented fibers by Sampson and co-workers, the pore size distribution is characterized by the coefficient of variation of pore radii for random networks, CV(r_{2D}) and parameters b and k[17,20,23]

$$CV(r_{2D}) = \frac{\sqrt{16-\pi^2}}{\pi} \quad (2)$$

$$CV(r_{2D}) = \frac{1}{\sqrt{k}} \quad (3)$$

$$\bar{r}_{2D} = k/b \quad (4)$$

Note that for current UF and MF membranes, a log-normal distribution of pore sizes is assumed (modeled by equation 6b). The assumption of a gamma distribution (equation 6a) is a fundamentally different approach to modeling pore size distribution and leads to a unique selectivity-permeability profile for nanofibrous filtration materials. **Figure 3** shows the difference in the pore size distribution for the two models, the gamma-type has a greater spread with a tail at the lager pore size end due to the higher coefficient of variation (CV) of ~0.8 (coefficient of variation is the ratio of standard deviation/mean) versus the log-normal distribution which has a CV of 0.2. [24] The higher CV for the gamma type pore size distribution is based on the analysis by Corte and Lloyd [23] for random networks as given by equation (2).

The number of layers of fibers (n) corresponding to desired porosity (ε), fiber diameter (ω), linear density (δ, g/m) and mean areal density of the network (β, g/m^2) is then given by [17]

$$n = \frac{\beta\omega}{\delta log(1/\varepsilon)} \tag{5}$$

where, linear density (δ, g/m) is the mass per unit length of fiber given by the product of material density (ρ) times the fiber cross sectional area

This results in a gamma type pore size distribution given by [17]

$$f(r) = \frac{n}{\epsilon}\left(\frac{\Gamma(k,br)}{\Gamma(k)}\right)^{(n/\varepsilon)-1} \frac{b^k}{\Gamma(k)} r^{k-1} e^{-br} \tag{6a}$$

The log-normal pore size distribution is given by [9]

$$f(r) = \frac{1}{r\sqrt{2\pi}}[ln(1+CV^2)^{-\frac{1}{2}}\, exp\left\{-\frac{\left(ln\left(\frac{r}{\bar{r}}\right)(1+CV^2)^{\frac{1}{2}}\right)^2}{2\, ln\,[1+CV^2]}\right\}] \tag{6b}$$

The average pore size ($\bar{r}$) of this distribution is given by [17]

$$\bar{r} = \int_0^\infty r f(r) dr \tag{7}$$

The thickness of the membrane (δ_m) can be calculated by using diameter of fiber (ω) and number of layers of fibers (n) as [17]

$$\delta_m = n\omega \tag{8}$$

Permeability

The expected permeability (L_p) using the probability distribution function and the Hagen Poiseuille relation for a membrane of thickness, δ_m is given by [9]

$$\overline{L_p} = \frac{\varepsilon}{8\mu\delta_m}\frac{\int_0^\infty f(r)r^4dr}{\int_0^\infty f(r)r^2dr} \quad (9)$$

where μ is the viscosity of water.

Selectivity

The selectivity (α) for a UF/MF membrane is given by [9]

$$\alpha = \frac{1}{S_a} \quad (10)$$

where S_a is the intrinsic separation factor of the membrane which can be evaluated by [9]

$$S_a(r) = (1-\lambda)^2[2-(1-\lambda)^2]exp\,(-0.7146\lambda^2) \quad (11)$$

where $\lambda = a/r$; a is the radius of the solute and r is the radius of the pore.

The overall sieving coefficient of the membrane is given by [9]

$$\overline{S_a} = \frac{\int_0^\infty S_a(r)f(r)r^4dr}{\int_0^\infty f(r)r^4dr} \quad (12)$$

The selectivity, $1/\overline{S_a}$ and permeability, L_p, for various conditions of membrane thickness, δ_m can be thus plotted to predict the performance of nanofibrous membranes and compared with the upper bound determined by Mehta and Zydney[9] or with the MF upper bound developed in this work.

The analysis was carried by assuming different fiber diameters and membrane thicknesses as well as material density. The model solute used for determination of selectivity for UF applications was bovine serum albumin (BSA) which has a radius of 3.65 nm[9] while that for MF applications was polystyrene particles with a radius of 0.1 μm.

Materials and methods

The selectivity and permeability of three different commercial MF membranes were determined in a stirred cell set-up. Specifically, these experiments employed Durapore polyvinylidene fluoride (PVDF) membranes, Millipore Express PLUS polyethersulfone (PES) membranes, and MF-Millipore mixed cellulose esters membranes. A 25 mm Amicon stirred cell (Model 8010) was connected to a reservoir of the solution to be filtered. For the water permeability experiments, this was nanopure water, and for the selectivity experiments, this was a 0.1 μm diameter blue fluorescent ThermoFisher FluoSpheres (carboxylated-modified microspheres) polystyrene particle solution at concentrations of 10^7-10^8 particles/mL. Approximately 500 μL of waste was collected to wash out the dead volume before collecting 500 μL of sample at constant pressure of 2 psi. The water permeability of all three systems was also measured before and after the filtration experiments. Differences in water permeability were less than 20%, indicating an absence of irreversible fouling of the membrane during filtration experiments. The particle concentrations of the collected samples were determined from a calibration curve of derived particle count rate, analyzed via a Malvern Zetasizer Nano ZS 90 dyanmic light scattering (DLS) system, versus known initial particle concentration (**Figure S1**, SI).[25]

Results and Discussion

The pore size, pore size distribution and active layer thickness of current UF and MF membranes are primary determinants of their most important transport parameters – permeability to solvent and selectivity for specific solutes (**Table 1**, detailed data in Supplementary Information Tables S1-S3). We ran a series of sensitivity tests on the model developed for fibrous mat membranes to determine the influence of each parameter on mat properties. The pore diameter versus fiber diameter was plotted over a range of membrane thicknesses / areal densities to verify that the model had been reproduced successfully (**Figure 4**) from a previous study by Sampson *et al*.[17,20,23] For a specific membrane thickness and areal density, we observed an increase in pore size with increasing fiber diameter due to fewer number of fibers deposited per unit area. We also observed that for a given fiber diameter, the pore radius is larger at lower membrane thickness. Also, the increase in effective pore radius with fiber diameter is a stronger function of fiber diameter for lower versus higher thickness membranes. This is because a given mat thickness would require more layers of thinner fibers than thick ones leading to greater

overlap/intersection between the pores of one layer and the walls of the adjacent one which in turn leads to smaller pore size and greater selectivity.

We also varied mat porosity and density at fixed mat thicknesses to observe the change in the selectivity- permeability performance of resulting membranes of varying fiber diameters. From the model developed, we observe that nanofiber mats with densities in the order of ~1.5 g/cm^3 and of thickness greater than 0.55 μm underperform in terms of selectivity in comparison to commercial UF filters at similar permeabilities (**Figure 5**). We also observe relatively low dependence of membrane performance on the mat porosity and density of the fibers except at low mat thickness, in which case lower density leads to improved mat selectivity for corresponding values of permeability.

Fibrous mat membranes for UF applications

For comparable porosities and material densities, electrospun membranes only outperform existing selectivity-permeability upper-bound of commercial UF / MF membranes for low membrane thicknesses. In fact, for porosities in the range of 0.9 and material densities of 0.094 g/cm^3, comparable to those of single-walled carbon nanotubes (SWCNTs), we would need membranes as thin as 100 nm to surpass the selectivity-permeability trade-off for UF applications (**Figure 6A**). Thus, depending on the material used, UF membranes with selectivity that surpass the upper bound of selectivity and permeability trade-off for commercial membranes may be obtained. However, for membrane thickness greater than 50 nm, there is a significant drop in permeability which causes the membrane selectivity-permeability performance for BSA to drop below the existing trade-off (**Figure 6A**).

In addition to being very thin, ~100 nm mats, the fibers used to deposit the mat have to be of low diameters, in the order of a few nanometers, ~2 nm to outperform conventional UF membranes (**Figure 7A**). For fibers with higher diameters, the selectivity drops while permeability increases as observed from the blue trace. For thicker fibers of the same material, fewer layers will be needed to construct a membrane of the same thickness, thus there would be fewer intersections which would lead to a membrane with a larger average pore size and lower solute retention. Thus the fiber diameter is a critical parameter in determining membrane performance. However, the

lower limit of fiber diameter produced by current electrospinning technologies is about 10 nm or higher. This puts a physical constraint on the use of electrospun polymer fibers- a suitable alternative may be cellulose, chitin or CNT nanofibers. CNTs of this size range (0.7-5 nm) can be produced, even though pure sub 2 nm SWCNTs are challenging to synthesize.[26] Cellulose nanofibers could be expected to have a limit of ~3 nm based on the size of a single crystalline cellulose microfibril.[27]

Additionally, very thin ~100 nm mats of CNT or cellulose would need to be mechanically robust with high compressive strength to be used for filtration purposes. Estimation and reports of Young's moduli and ultimate strength indicate that if such a layer of cellulose nanofibers and CNTs can be produced then its strength may be comparable or higher than current UF membranes (summarized in **Table 2**). The higher moduli and strength of nanofibers is not unusual as both cellulose and CNTs are known to have higher moduli and strength compared to conventional polymeric materials. Further, in terms of fiber modulus, lower fiber diameters are reported to have higher tensile strengths.[28] This is advantageous for the application of thin nanofibrous mats as filtration materials. Additionally according to the well-known Weibull's correlation, a small volume of interconnected fibers will have a higher ultimate strength, as strength is inversely correlated to volume, indicating the challenge of maintaining strong bonds between fibers as the number of bonds increase.[29] Thus from the perspective of strength and compressibility, having a thin submicron layer of nanofibers is advantageous.

Electrospun membranes for MF applications

We determined the permeability and selectivity performance of commercially available MF membranes using filtration experiments with polystyrene beads of 0.2 μm diameter (**Figure 2**). Our results show that the commercial membranes outperform the literature reported electrospun membranes which can be largely attributed to the broader gamma- based pore size distribution of electrospun membranes compared to the tighter log-normal distribution of phase-inversion based MF membranes. Similar to UF membranes, electrospun membranes can potentially outperform MF upper bound if very thin membranes, thinner than 0.74 μm are cast with fibers diameters of about ~70 nm (**Figures 6B, 7B**). Fiber diameters in the order of ~100 nm can be easily achieved by a variety of polymers, including PVA, PAN, PVDF by optimizing applied voltage, solution

composition and hence, viscosity, and other electrospinning conditions.[6-8] However, the sub-micron mat thickness requiredis orders of magnitude lower than typical nanofibrous mats reported in literature (10– 180 microns). [6-8,30]

High performance nanofibrous mat MF membranes

According to our model, only very thin low diameter electrospun membranes that are challenging to obtain with existing technologies will outperform conventional MF membranes. However, instances of high performance ~10 um thick electrospun MF membranes have been reported in literature (**Figure S2**, SI). Examples include the m-aramid class of membranes formed by electrospinning N,N-Dimethylacetamide (DMAc) in presence of $CaCl_2$.[31] Salts interact with DMAc leading to an increased charge density, which coupled with higher applied voltage leads to generation of thin ~120 nm fibers. In addition to thin fibers, electrospinning also generates nano-fiber branches of 10-25 nm which result in a nano-mesh structure with improved selectivity for particles.[31] Other examples include water-soluble PVA membranes of ~10 um thickness which are crosslinked post casting to render them suitable for aqueous phase filtrations.[6] The high surface area to volume ratio, open and highly interconnected pore structure of the membrane results in 1.5 to 6 fold improvement in permeability over commercial MF membranes. This is because commercial MF membranes formed by phase inversion have greater number of dead end pores along the depth of the membranes leading to lower permeability especially for thicker membranes, with typical thickeness in the ~ 30 -150 micron range.[30] In addition to the higher permeability, these membranes also have higher selectivity. This improvement is attributed to hindered movement of particles along the depth of the mat and laterally between adjacent layers of the mat. Thus, two parameters that dictate the ease of particle movement and hence, the selectivity are the number of layers and distance between adjacent layers; the higher number of layers comprising a nanofibrous mat and the smaller the inter-layer distance the greater the selectivity.

Conclusions

Overall, while nanofibrous mats created using electrospinning have created a new class of materials that are now poised to be applied to a wide variety of fields, its application to UF and

MF may not necessarily provide a large improvement in performance before a few engineering challenges can be overcome. For electrospun membranes to outperform existing MF membranes, the major requirements are 1) fibers (of ~100 nm diameter) which may be readily obtained with a range of polymers and electrospinning conditions, and 2) very thin robust defect-free mats (of ~ <1000nm in diameter) which may be challenging to obtain with existing technologies. The major challenges to using electrospun membranes for UF include 1) the need to produce very thin (~ 100 nm) layers of nanofibers, and 2) the need to use small diameter nanofibers (~ 2 nm) to create such layers. These limit the materials that could be used for such membranes using currently available technologies.

Acknowledgements. The authors would like to thank Prof. Andrew Zydney for helpful comments.

Supporting Information. The Supporting Information is available free of charge on the

ACS Publications website at DOI: xxx

Figures S1- S2, Tables S1- S3

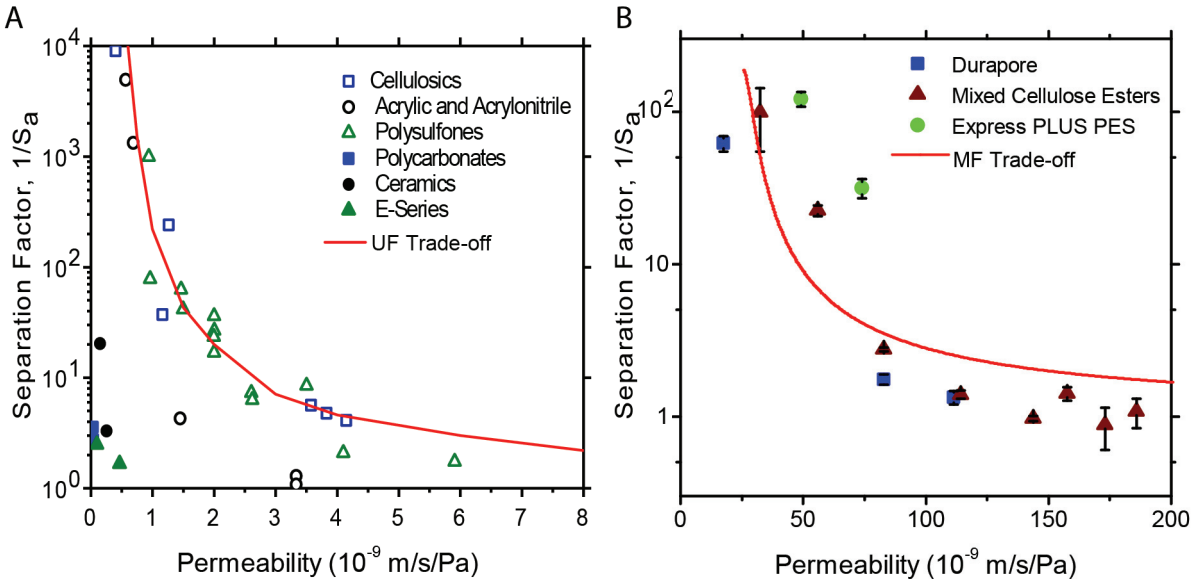

Figure 1. Upper bound for UF and MF membranes representing the trade-off between selectivity and permeability for log-normal pore size distribution. This provides a baseline for comparison of new membrane filtration materials. **A.** Trade-off for UF membranes based on BSA as model solute as proposed by Zydney and co-workers[9]. (Copyright permission pending) **B.** Trade-off for MF membranes based on experiments with 0.2 μm diameter microspheres as model solute. The curve shown is an arbitrary fit to the data points using a log normal pore size distribution assuming porosities of 80% and thickness of 3.9 μm.

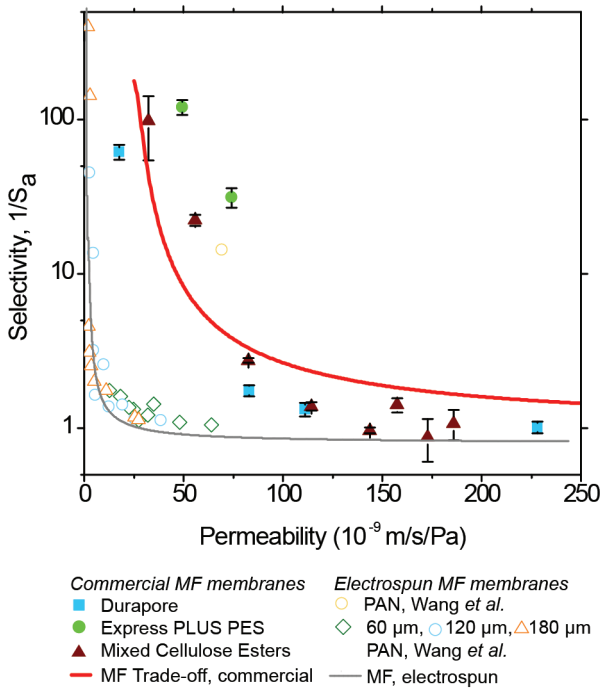

Figure 2. Permeability-selectivity performance of literature-reported electrospun membranes for MF applications. Electrospun membranes show much lower permeability-selectivity upper bound (gray trace) for 0.2 µm diameter microspheres than conventional MF membranes (red trace). As can be seen from the data, electrospun membrane performance for a reference set of polyacrylonitrile membrane[7] can be predicted by assuming a gamma pore size distribution for a membrane thickness of 60 µm and porosity of 0.8 which is similar to the parameters reported for these representative electrospun fibrous mat membranes in literature. The lower selectivity of electrospun membranes is attributed to their larger pore size and broader pore size distribution compared to conventional MF membranes of similar order of magnitude thickness and porosity (0.8) This greater deviation from mean pore size for electrospun membranes is because while conventional membranes formed by phase inversion follow a log-normal pore size distribution, membranes randomly deposited to form a fibrous mat of comparable thickness have pore sizes that follow a gamma distribution.

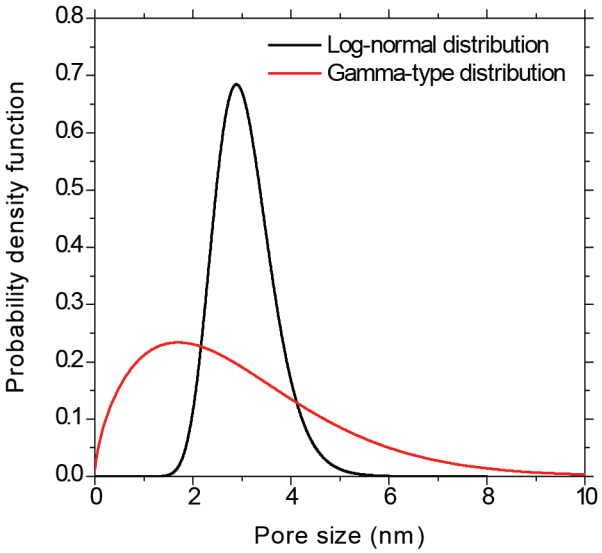

Figure 3. The pore size distribution varies dramatically between the log-normal size distribution used for current UF membranes and the proposed gamma pore size distribution for fibrous mats. While the log-normal distribution has a much smaller spread due to its lower coefficient of variation (i.e., the ratio of standard deviation to mean) we see a much wider spread for the gamma distribution due to the higher CV for the same mean pore size. The log-normal distribution was based on a 30 kDa ultrafiltration membrane with a pore size of ~3.3 nm [24] and a coefficient of variation of 0.2 while the nanofibrous gamma-type was based on a system with much higher CV of ~0.8.

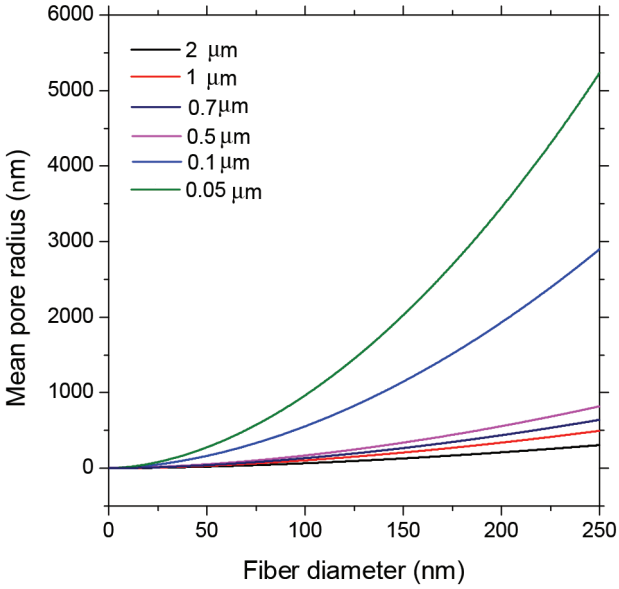

Figure 4. Pore diameter becomes a stronger function of fiber diameter as the thickness of the fibrous mat membrane decreases. For the same areal density, the decrease in fiber diameter leads to a decrease in mean pore radius, the increase being much greater for lower thickness mats. The data presented here is identical to a similar figure in Eichhorn and Sampson [17,20,23] indicating that we have successfully reproduced the model.

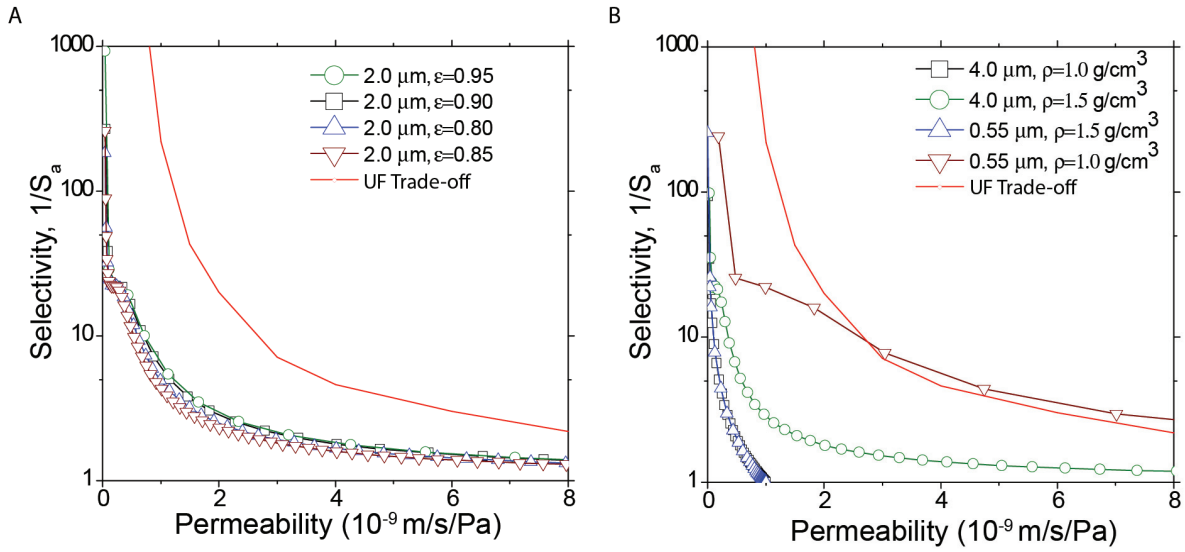

Figure 5. Porosity (ε) has a negligible effect (A) while density (ρ) of fibers has a stronger influence (B) on the permeability-selectivity performance of nanofibrous membranes for comparable thicknesses. The effect of density is more pronounced at lower membrane thickness; greater selectivity is observed for lower versus higher density fibers at 0.55 µm thickness (the thickness used in the upper bound calculations for current UF membranes).

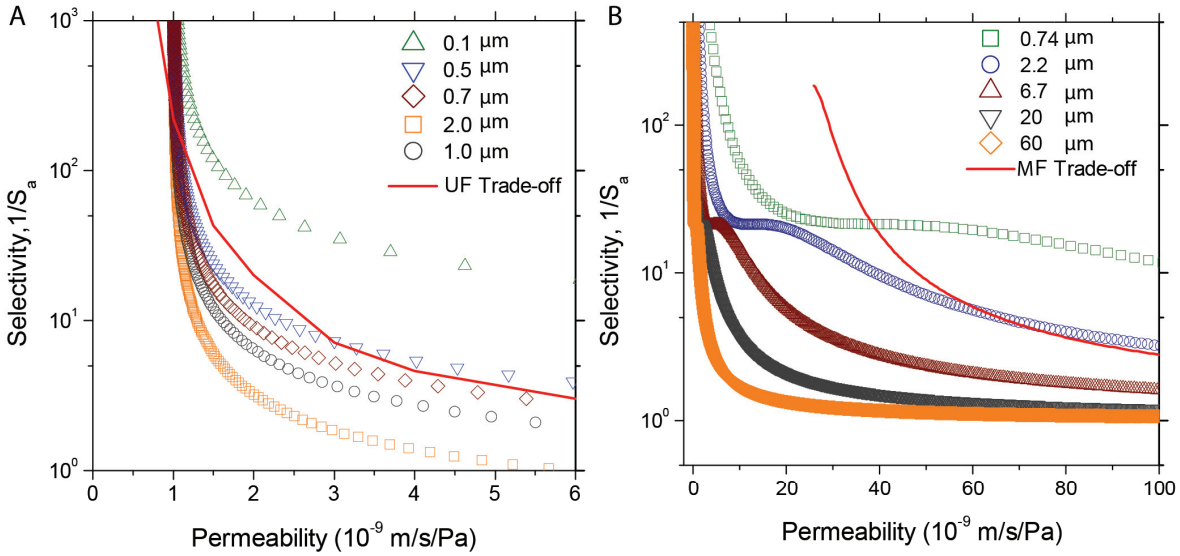

Figure 6. Only electrospun membranes of relatively low thickness and fiber diameter can outperform commercially available MF and UF membranes. A. Ultrathin layers of thin nanofibers will be required for fibrous or electrospun mats to exceed the performance of current UF membranes. Selectivity-permeability trade-off curves for nanofibrous mats show that fibrous mats can outperform the commercial UF membrane only at membrane thicknesses below ~ 0.1 μm. At the low permeability and the high selectivity region, the mat construction has to be with very thin fiber diameters as shown in Figure 7A. The density used in these calculations was 0.094 g/cm^3 which is characteristic of SWCNTs which are typically 0.7-5 nm in diameter. Most nanofibrous membranes that are thicker are predicted to perform less effectively than commercial UF membranes, i.e., for comparable selectivities to soluble protein, BSA, their permeabilities would be lower according to the Hagen Poiseuille equation. **B. Electrospun membranes of very low thickness but reasonable fiber diameters can potentially outperform commercially available MF membranes.** Typically MF membranes thinner than 0.74 μm are required to outperform MF selectivity- permeability upper-bound. As observed in Figure 7B, for a membrane of thickness 0.74 μm and porosity of 0.9 fiber diameters of about 67 nm diameter will be required. Fiber diameters of ~70 nm can be obtained by electrospinning polyacrilonitrile (PAN) which has a density of 1.184 g/cm^3 which was used to model the selectivity – permeability of MF membranes. However, to outperform MF membranes would require relatively defect-free thin mats under 740 nm which may be challenging to obtain using conventional electrospinning techniques. The distinct shape of the curves is a direct consequence

of the gamma type pore size distribution used for nanofibrous media that has a long “tail” at the larger pore sizes compared to the log-normal pore size distribution used for phase inversion UF/MF membranes.

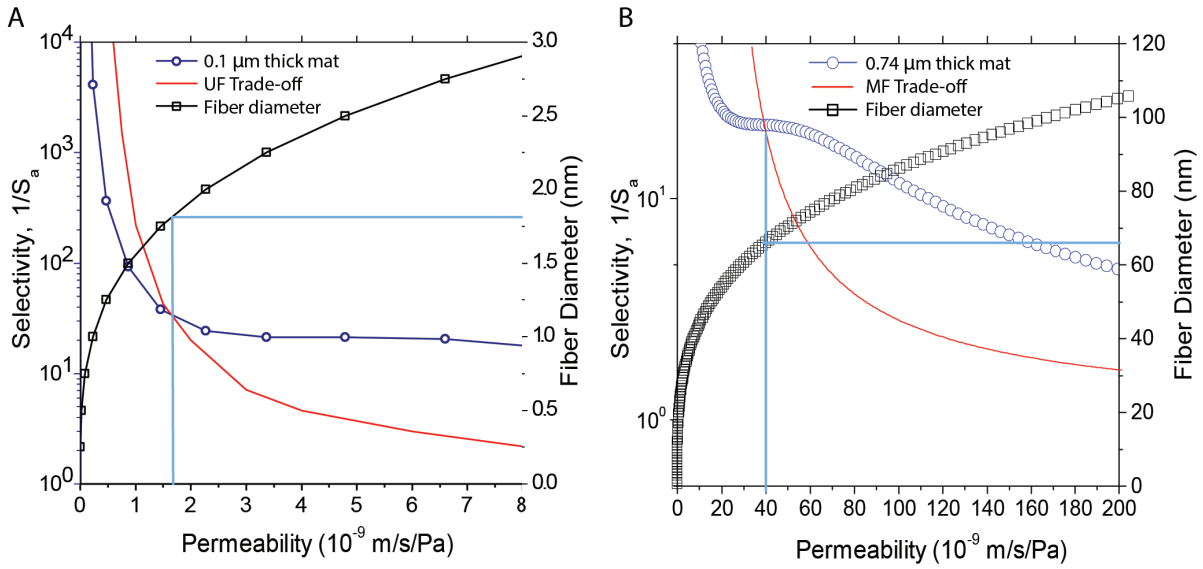

Figure 7. Fiber diameters needed for synthesizing the 0.1 µm and 0.74 µm thick nanofibrous mats which may outperform current commercial UF and MF membranes respectively (red traces in panel A and B). Improved performance is obtained when the selectivity-permeability for the nanofibrous mats from the model (navy blue trace) intersects the proposed upper limit of selectivity-permeability trade-off (red trace) as marked by the vertical light blue line and offers greater selectivity for corresponding permeability values. The minimum fiber diameter at which the nanofibrous mats outperform the commercial ones is marked by the intersection of the light blue vertical line with the fiber diameter versus permeability trace (black). Thus to obtain high enough selectivity we require relatively low fiber diameters. Using thicker fibers for the same thickness mat would cause us to move further along the selectivity-permeability curve (navy blue) leading to higher permeability at a loss of selectivity. Here, we represent mats of 2 different thicknesses for UF and MF applications. **A.** Electrospun membranes that outperform UF membranes would have to be of fiber diameter >1.7 nm for 0.58 nm pore diameter, and 0.1 µm thick with a permeability of 1.5×10^{-9} m/s/Pa and selectivity of ~40 for 3.65 nm radius BSA molecules. **B.** Electrospun membranes that outperform MF membranes would have to be of fiber diameter >67 nm (or less than 10 layers) for 24 nm pore diameter and 0.74 µm thick with a permeability of 40×10^{-9} m/s/Pa and selectivity of ~22 for 0.1 µm radius particles. In both cases the thickness of the fibers determines the number of layers required to construct a given thickness mat; thicker fibers would result in fewer layers which in turn leads to larger pore sizes and lower selectivity. The thinner of the two mats, case A, requires thinner fiber

diameters of lower density which may be obtained with SWCTs to outperform commercial UF membranes and also offers greater selectivity for a given solute size. The thicker mat, case B, which may be obtained with higher density and higher thickness PAN fibers is better suited for MF applications.

Table 1: Representative structural property and performance ranges of commercial UF and MF phase-inversion membranes. (see Supporting information Tables S1 to S3 for detailed information)

Solutes	Pore size (nm)	Permeability (10^9m/s/Pa)	Pore density	Porosity	Membrane thickness (μm)	
			(#/nm^2)	(%)	active layer	overall
Ultrafiltration						
5-1000 kDa	1.3-17	2.4-416	~10^{16}	8.3-66	.75-85	135-280
Microfiltration						
0.05-10 μm	25-10,000	7-186		60-85	30-150	

Table 2: Comparison of mechanical properties of nanofibers and nanofiber membranes to commercial membrane materials and membranes.

	fiber or material		membrane	
Membrane Material	Young's modulus (GPa)	Ultimate Strength (MPa)	Young's modulus (GPa)	Ultimate Strength (MPa)
Conventional Membrane Materials (Polyether Sulfone (PES), Cellulose Acetate (CA), Polyvinylidene Fluoride (PVDF))	0.08-4[32]	40-65[32]	1.3-4.2[32]	18-52[32]
Cellulose Nanofibers/Microfibers	50-143[33]	10,000[13]	15[33]	129-4[12]
Carbon Nanotubes (CNT)	67-1300[34]	11,00-63,000[35]	1.1-24[14]	6.3-57[14]

REFERENCES

(1) Renner, E.; Abd-El-Salam, M.: *Application of ultrafiltration in the dairy industry*; Elsevier Science Publishers Ltd., 1991.

(2) Hamza, A.; Pham, V.; Matsuura, T.; Santerre, J. Development of membranes with low surface energy to reduce the fouling in ultrafiltration applications. *Journal of Membrane Science* **1997**, *131*, 217-227.

(3) Vieira, M.; Tavares, C.; Bergamasco, R.; Petrus, J. Application of ultrafiltration-complexation process for metal removal from pulp and paper industry wastewater. *Journal of Membrane Science* **2001**, *194*, 273-276.

(4) Ciardelli, G.; Corsi, L.; Marcucci, M. Membrane separation for wastewater reuse in the textile industry. *Resources, conservation and recycling* **2001**, *31*, 189-197.

(5) Mohammad, A. W.; Ng, C. Y.; Lim, Y. P.; Ng, G. H. Ultrafiltration in food processing industry: review on application, membrane fouling, and fouling control. *Food and bioprocess technology* **2012**, *5*, 1143-1156.

(6) Liu, Y.; Wang, R.; Ma, H.; Hsiao, B. S.; Chu, B. High-flux microfiltration filters based on electrospun polyvinylalcohol nanofibrous membranes. *Polymer* **2013**, *54*, 548-556.

(7) Wang, R.; Liu, Y.; Li, B.; Hsiao, B. S.; Chu, B. Electrospun nanofibrous membranes for high flux microfiltration. *Journal of membrane science* **2012**, *392*, 167-174.

(8) Wang, Z.; Crandall, C.; Sahadevan, R.; Menkhaus, T. J.; Fong, H. Microfiltration performance of electrospun nanofiber membranes with varied fiber diameters and different membrane porosities and thicknesses. *Polymer* **2017**, *114*, 64-72.

(9) Mehta, A.; Zydney, A. L. Effect of membrane charge on flow and protein transport during ultrafiltration. *Biotechnology progress* **2006**, *22*, 484-492.

(10) Yoon, K.; Hsiao, B. S.; Chu, B. Functional nanofibers for environmental applications. *Journal of Materials Chemistry* **2008**, *18*, 5326-5334.

(11) Ding, B.; Yu, J.: *Electrospun nanofibers for energy and environmental applications*; Springer, 2014.

(12) Henriksson, M.; Berglund, L. A.; Isaksson, P.; Lindstrom, T.; Nishino, T. Cellulose nanopaper structures of high toughness. *Biomacromolecules* **2008**, *9*, 1579-1585.

(13) Hamad, W. On the development and applications of cellulosic nanofibrillar and nanocrystalline materials. *The Canadian Journal of Chemical Engineering* **2006**, *84*, 513-519.

(14) Berhan, L.; Yi, Y.; Sastry, A.; Munoz, E.; Selvidge, M.; Baughman, R. Mechanical properties of nanotube sheets: Alterations in joint morphology and achievable moduli in manufacturable materials. *Journal of Applied Physics* **2004**, *95*, 4335-4345.

(15) Barhate, R.; Loong, C. K.; Ramakrishna, S. Preparation and characterization of nanofibrous filtering media. *Journal of Membrane Science* **2006**, *283*, 209-218.

(16) Yoon, K.; Kim, K.; Wang, X.; Fang, D.; Hsiao, B. S.; Chu, B. High flux ultrafiltration membranes based on electrospun nanofibrous PAN scaffolds and chitosan coating. *Polymer* **2006**, *47*, 2434-2441.

(17) Wang, X.; Fang, D.; Hsiao, B. S.; Chu, B. Nanofiltration membranes based on thin-film nanofibrous composites. *Journal of Membrane Science* **2014**, *469*, 188-197.

(18) Eichhorn, S. J.; Sampson, W. W. Relationships between specific surface area and pore size in electrospun polymer fibre networks. *Journal of the Royal Society, Interface / the Royal Society* **2010**, *7*, 641-649.

(19) Eichhorn, S. J.; Sampson, W. W. Statistical geometry of pores and statistics of porous nanofibrous assemblies. *Journal of the Royal Society, Interface / the Royal Society* **2005**, *2*, 309-318.

(20) Sampson, W. A multiplanar model for the pore radius distribution in isotropic near-planar stochastic fibre networks. *Journal of materials science* **2003**, *38*, 1617-1622.

(21) Dodson, C.; Sampson, W. The effect of paper formation and grammage on its pore size distribution. *Journal of pulp and paper science* **1996**, *22*, J165.

(22) Sampson, W. Materials properties of paper as influenced by its fibrous architecture. *International Materials Reviews* **2009**, *54*, 134-156.

(23) Corte, H.; Lloyd, E. In *Tilte*1965.

(24) Mehta, A.; University, T. P. S.: *Performance Characteristics of Charged Ultrafiltration Membranes: Fundamental Studies and Applications*; Pennsylvania State University, 2006.

(25) Smeraldi, J.; Ganesh, R.; Safarik, J.; Rosso, D. Statistical evaluation of photon count rate data for nanoscale particle measurement in wastewaters. *Journal of Environmental Monitoring* **2012**, *14*, 79-84.

(26) De Volder, M. F.; Tawfick, S. H.; Baughman, R. H.; Hart, A. J. Carbon nanotubes: present and future commercial applications. *Science* **2013**, *339*, 535-539.

(27) Cosgrove, D. J. Re-constructing our models of cellulose and primary cell wall assembly. *Current opinion in plant biology* **2014**, *22*, 122-131.

(28) Wong, S.-C.; Baji, A.; Leng, S. Effect of fiber diameter on tensile properties of electrospun poly (ε-caprolactone). *Polymer* **2008**, *49*, 4713-4722.

(29) I'Anson, S.; Sampson, W. Competing Weibull and stress-transfer influences on the specific tensile strength of a bonded fibrous network. *Composites science and technology* **2007**, *67*, 1650-1658.

(30) http://www.emdmillipore.com/US/en/product/MF-Millipore-Membrane-Filter%2C-mixed-cellulose-esters,MM_NF-VCWP02500. (accessed 07/14 2017).

(31) Yu, J.; Kim, Y.-G.; Kim, D. Y.; Lee, S.; Joh, H.-I.; Jo, S. M. Super high flux microfiltration based on electrospun nanofibrous m-aramid membranes for water treatment. *Macromolecular Research* **2015**, *23*, 601-606.

(32) Arkhangelsky, E.; Kuzmenko, D.; Gitis, N. V.; Vinogradov, M.; Kuiry, S.; Gitis, V. Hypochlorite cleaning causes degradation of polymer membranes. *Tribology Letters* **2007**, *28*, 109-116.

(33) Tanpichai, S.; Quero, F.; Nogi, M.; Yano, H.; Young, R. J.; Lindstrom, T.; Sampson, W. W.; Eichhorn, S. J. Effective Young's modulus of bacterial and microfibrillated cellulose fibrils in fibrous networks. *Biomacromolecules* **2012**, *13*, 1340-1349.

(34) Salvetat, J.-P.; Briggs, G. A. D.; Bonard, J.-M.; Bacsa, R. R.; Kulik, A. J.; Stöckli, T.; Burnham, N. A.; Forró, L. Elastic and shear moduli of single-walled carbon nanotube ropes. *Physical review letters* **1999**, *82*, 944.

(35) Yu, M. F.; Lourie, O.; Dyer, M. J.; Moloni, K.; Kelly, T. F.; Ruoff, R. S. Strength and breaking mechanism of multiwalled carbon nanotubes under tensile load. *Science* **2000**, *287*, 637-640.